10

ANALYTICAL TRAUMA RESEARCH USING THE CHEST BAND

Nopporn Khaewpong
Chi Associates, Inc.
Arlington, VA

Rolf H. Eppinger
Richard M. Morgan
National Highway Traffic Safety Administration
U.S. Department of Transportation
Washington, DC
USA

October 2, 1991

This paper was presented at the 19th Annual Workshop on Human Subjects for Biomechanical Research. It has not been screened for accuracy nor refereed by any body of scientific peers and should not be referenced in the open literature.

National Highway Traffic Safety Administration
U.S. Department of Transportation
400 Seventh Street, SW
Washington, DC 20590
USA

Tel: 202-366-4704
Fax: 202-366-5670

Analytical Trauma Research Using The Chest Band

Nopporn Khaewpong — Chi Associates, Inc., Arlington, VA, USA

Rolf H. Eppinger, Richard M. Morgan — National Highway Traffic Safety Administration, U. S. Department of Transportation, Washington, DC, USA

Abstract

This paper explores the potential for developing improved thoracic injury criteria using data derived from experiments using the chest band. The chest band is both a sensing device and an analytical process that determines the cross-sectional geometry of an object about which it is wrapped. In the process of determining the geometric shape of the object, the chest band process also provides both the local curvature and the time rate of change of the curvature of the object's peripheral surface. Thus the time histories of these variables at both fracture and non-fracture sites can be documented. A discussion of the rationale and the methodology for relating local curvature and other factors with thoracic skeletal injury is provided. Additionally, the rationale and processes of using the derived time varying contours from the chestband to establish the extent of internal thoracic injury are also explored by using a simplified finite element model of the chest. This model is a one-inch thick viscoelastic material in the shape of the measured thoracic contour. It is stimulated by using the time varying external contours obtained from the chestband as the inputs to calculate the stress and strain distribution throughout the model. Initial analysis indicates that the stresses and strains internal to the body are produced not only by the deformation of the periphery but are also influenced by the inertial conditions to which the entire body is exposed while being deformed.

Introduction

The External Peripheral Instrument for Deformation Measurement (EPIDM), or the more commonly called chest band, is both a sensing device and an analytical process that determines the cross-sectional geometry of a body about which it is wrapped. The sensing device consists of a urethane-encapsulated metallic strip to which a number of strain gauge bridges are attached at various locations along its length. These sensors are configured to sense local curvature of the band. The output from the physical chestband is the time histories of the curvature at multiple points on the periphery of the thorax

around which the chestband is wrapped. Figure 1 shows a typical curvature time history during an impact event recorded by one of the strain bridges on the band. A continuous description of the curvature, K, around the periphery of the band (and body) at any instant in time, as shown in Figure 2, is approximated by an analytical fitting process, [1], that uses the multiply measured discrete curvatures obtained from the physical band. Typically, the bands used in the current experimental series have had either 16, 24, or 40 individual bridges around the periphery. The reconstruction of the band's (and the body's) geometry is then performed using the continuous curvature information and an example of this process is shown in Figure 3.

Figure 1. Curvature Time History

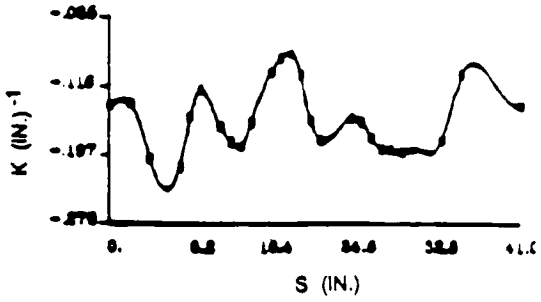

Figure 2. Distribution of curvature around Thorax

Thoracic Skeletal Injury

While skeletal injury can obviously occur throughout most of the body, detection and accurate prediction of the location and extent of skeletal injury in the highly deformable thoracic area has proven most elusive. Both field and laboratory studies have shown that thoracic skeletal injuries occur not only at sites where the crash forces are applied but at sites remote from the application of force. This evidence together with the observations that the thorax undergoes significant deformation during an impact suggests that rib failure is primarily a result of bending. Therefore, the following discussion develops a rationale and proposes a process that utilizes the time changing geometric information provided by the chest band to detect conditions of fracture on the thoracic structure. It is anticipated that the actual critical threshold values for fracture will be empirically derived from a series of laboratory experiments simulating frontal impacts using a variety of different restraint systems (Airbag, three-point belt, etc.) using the rationale and methodology discussed herein. An assessment of how the early experimental results support the proposed criterion is also presented. These early results were obtained using 16-gauge bands and further experimentation will be needed using higher-density gauge bands which have been shown to provide more accurate results. [8]

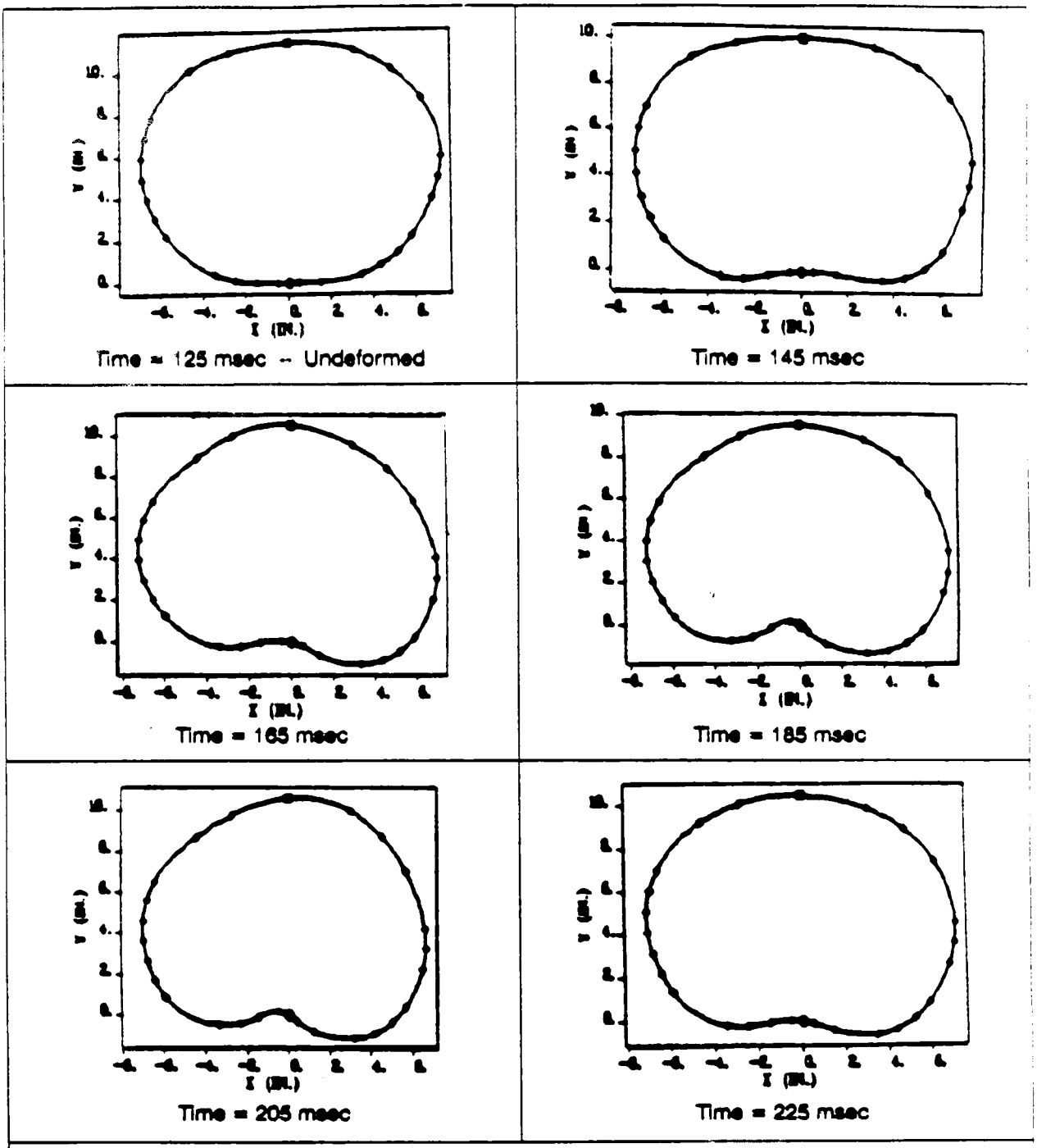

Figure 3. A series of chest contours captured by the chestband.

Proposed Thoracic Fracture Criterion

If one assumes that the ribs of the thorax are primarily vulnerable to failure in bending and that their geometric configuration prior to impact is strain free, then the prospect of failure at any point on a rib should be a function of the difference between the deformed curvature at that point and the original curvature at that point regardless of the type of external loading and the rib's material and failure properties. Since each location along the length of a rib could experience either a positive or negative change in curvature depending on the type of loading experienced during an impact and since it is highly likely that the ribs have a variety of nonuniformities, the critical change in curvature that identifies the onset of local fracture may be different for positive and negative changes of curvature. As a result, it is anticipated that both parameters will have to be monitored. If the influence of the nonuniformities is small, then the absolute value of the change in curvature may be a sufficient indicator of fracture potential. Additionally, since the architecture of the rib's cross-section varies both along its length and possibly in the vertical direction, the critical change in curvature values may also vary along the rib's length and as a function of elevation.

Since the ultimate objective is to predict rib fracture risk for an entire dynamic event, the maximum change in curvature, be it positive, negative, or absolute, over the entire event is proposed as the parameter that should be the most descriptive of fracture. Figure 4 illustrates a typical, complete distribution of curvature around the thorax of a cadaver undergoing an impact test in a belt restraint at two different times: one just prior to the application of forces (at a time of 112.5 milliseconds on the event clock) and one 38 milliseconds later. The difference between these two curves, shown in Figure 5, represents the strain induced into a rib structure at that instant in time and, therefore, is the parameter that should be indicative of rib failure potential at that time.

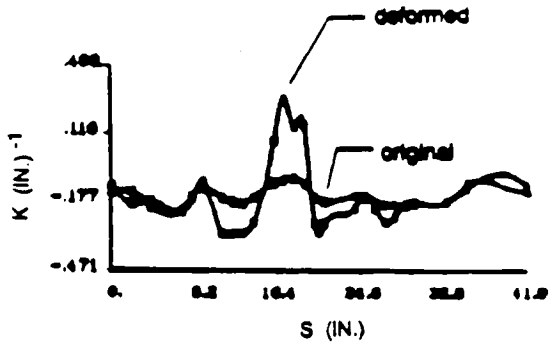

Figure 4. Thoracic Curvatures associated with original and deformed states

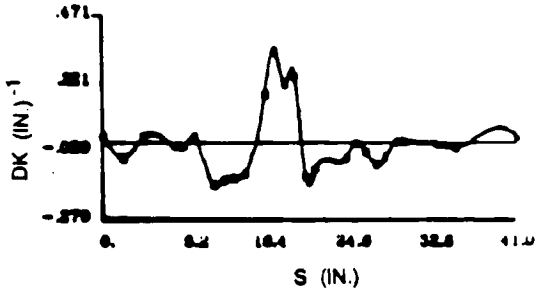

Figure 5. Change in curvature due to deformation of thorax

The absolute maximum change of curvature, Max. DK, along the total peripheral length of the structure for the entire event is shown in Figure 6a while the maximum positive and negative changes are shown in Figures 6b and 6c respectively.

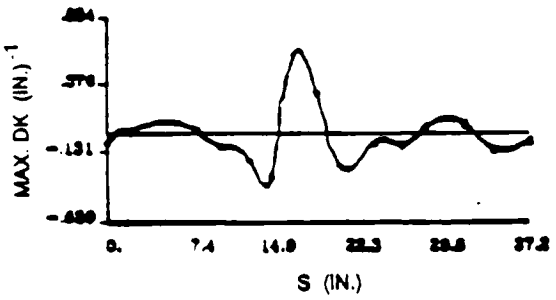

Figure 6a

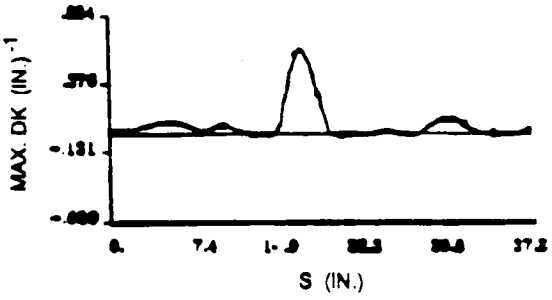

Figure 6b

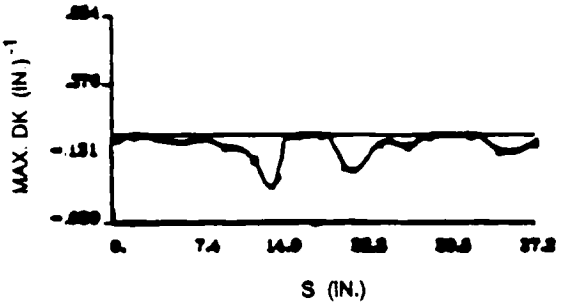

Figure 6c

Figure 6a. Absolute max change of curvature along the band length S

Figure 6b. Positive max change of curvature along the band length S

Figure 6c. Negative max change of curvature along the band length S

A hypothesized fracture tolerance level for absolute maximum change of curvature is shown in Figure 7. In this figure, the curvature is depicted starting at the spine, S = 0 inches, and proceeding around the thorax to the left until coming to the sternum, s = 19 inches, and then continuing around to the right until the spine is again encountered, S = 40 inches.

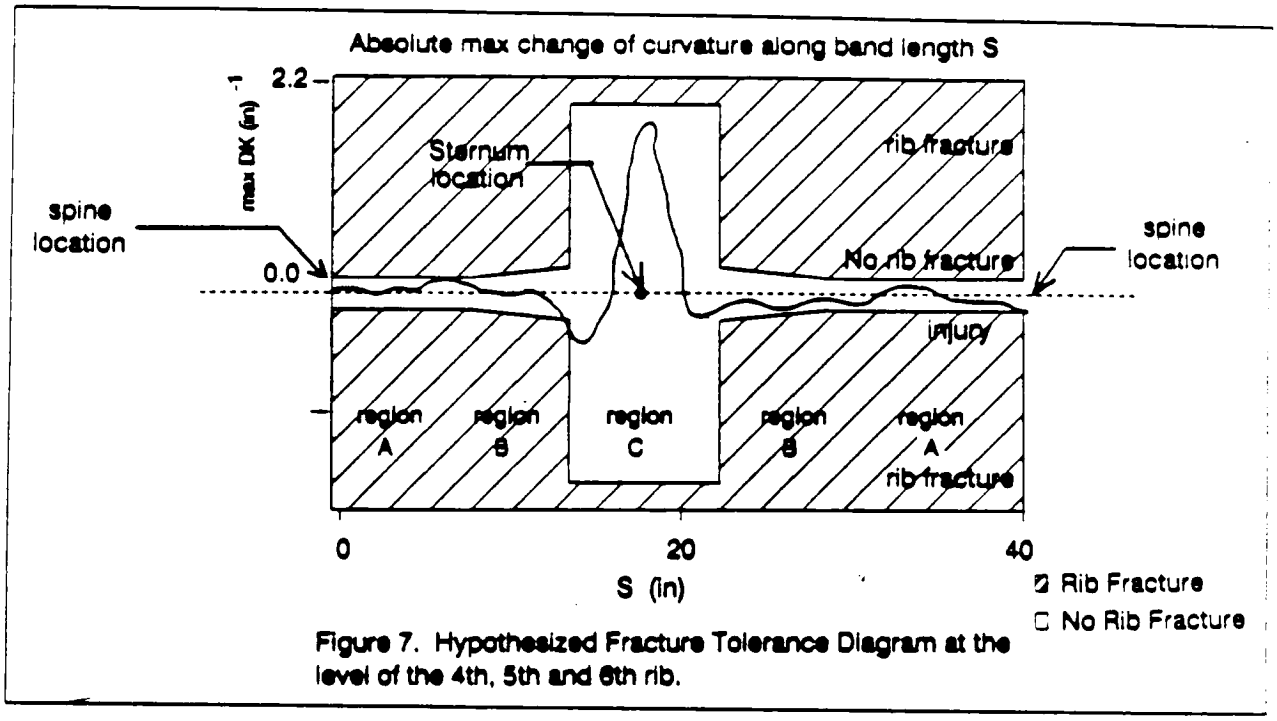

Figure 7. Hypothesized Fracture Tolerance Diagram at the level of the 4th, 5th and 6th rib.

To compensate for possible geometrical and material changes in the rib structure along its length, the critical change in curvature is envisioned to be different for three different regions, as depicted in Figure 8, around the thorax: Region A covers the area 5 inches on either side of the spine, region C covers the area approximately 4 inches on either side of the sternum and represents the cartilaginous portion of the thorax, and region B, the rib structure connecting the two other regions.

The curvature change for fracture onset is depicted as very small for Region A. The reasoning being that the greater section modulus in this area would cause critical tensile failure stresses to be reached with less curvature change than in region B. Region B has a somewhat higher critical value because of the expected smaller section modulus which requires a greater change in curvature to achieve the same surface stresses in the rib. Region C's very high critical value is reasoned to exist because of the cartilaginous nature of the material of the sternal area which would be very flexible and require a much greater change in curvature before failure would occur. In addition to the variation of the fracture threshold curvature in the circumferential direction, it is possible that the fracture threshold values of maximum change of curvature may also vary in the vertical direction. Strictly speaking, it should be assumed that the tolerance

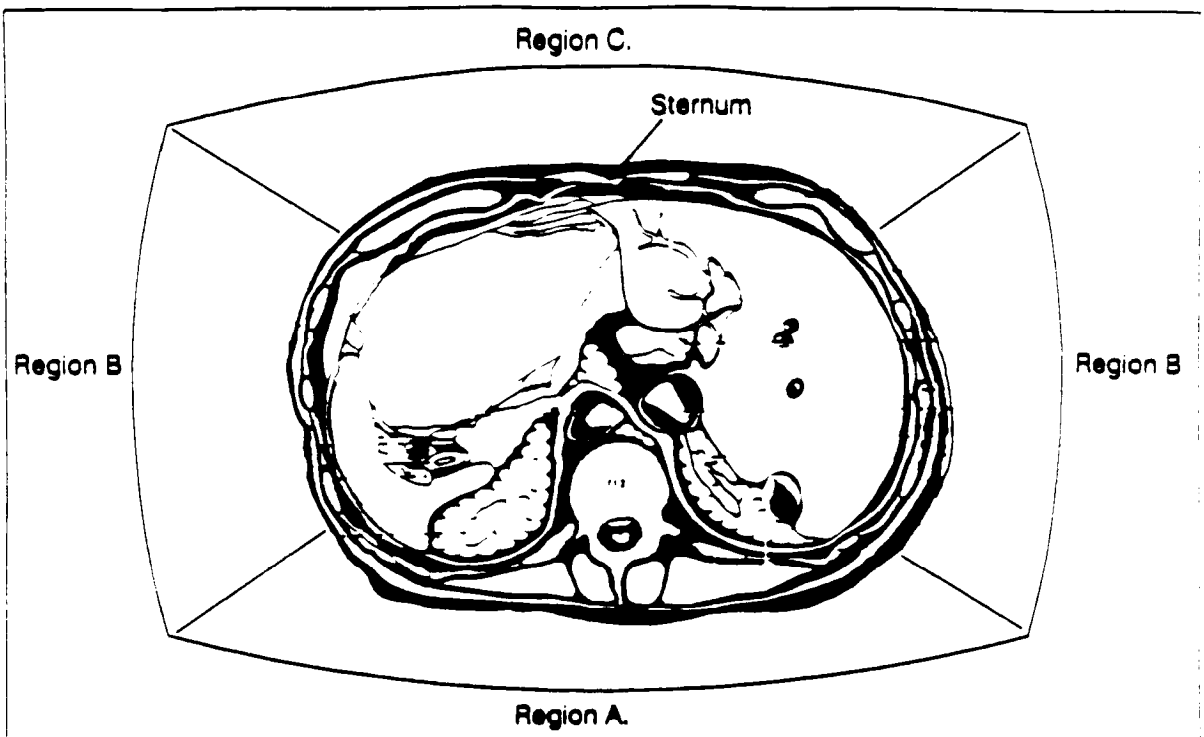

Figure 8. Subregions with common Fracture Tolerance in the Circumferential Direction

level of the maximum change of curvature would vary continuously in the vertical direction. As with the circumferential variation, it is probably necessary to simplify these vertical variations into a limited number of regions with common threshold values within each. In this case however there are no obvious physical differences which would permit a reasonable ex ante classification to be made. Therefore, as a starting point, the threshold variation in the vertical direction could be explored by separating the thorax into possibly three vertical regions as shown in Figure 9, if the resulting experimental data allows.

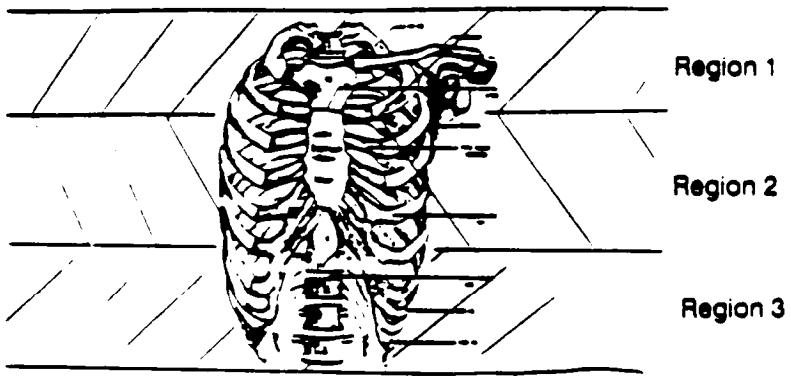

Figure 9. Subregions with common Fracture Tolerance level in Vertical (Superior-Inferior) Direction

The material properties of the bone obviously have a significant influence on the condition at which failure occurs. Since the strength of human bones changes with age [2], it is reasonable to expect that the tolerance level of an older individual would be less than that of a young individual. How much the age factor contributes to the change in tolerance when considering curvature change is still unknown. It is possible that the standard deviation of the age factor is much less than those of the fracture location. In that case the age factor could be dropped from the criterion. But if the opposite is true then the tolerance level chart (similar to Figure 7) would become more complex. This would also be true for both the circumferential and vertical directions.

Experimental Results

Two frontal impact sled tests of cadavers restrained by three point-belt restraints have been conducted. The change in velocity of both tests was about 30 MPH. In the first test, performed by the Medical College of Wisconsin (MCW), the cadaver was 73 years old. A 36-gauge and a 16-gauge chest bands were used at level 5 and 7 respectively (see the diagram in Figure 10). The autopsy summary indicates that rib fracture occurred at ribs number 2,3,4,5,7and 8 at the midportion of the ribs. In addition rib 4 also had a second fracture at 3.5 cm lateral from midsternum. The absolute maximum change of curvature along the band length, i.e Max. DK vs. S curve, for both bands is shown in Figure 11. Figure 10 shows that the top band was located at the level of ribs 4 and 5 while the bottom band was at the level of ribs 7 and 8.

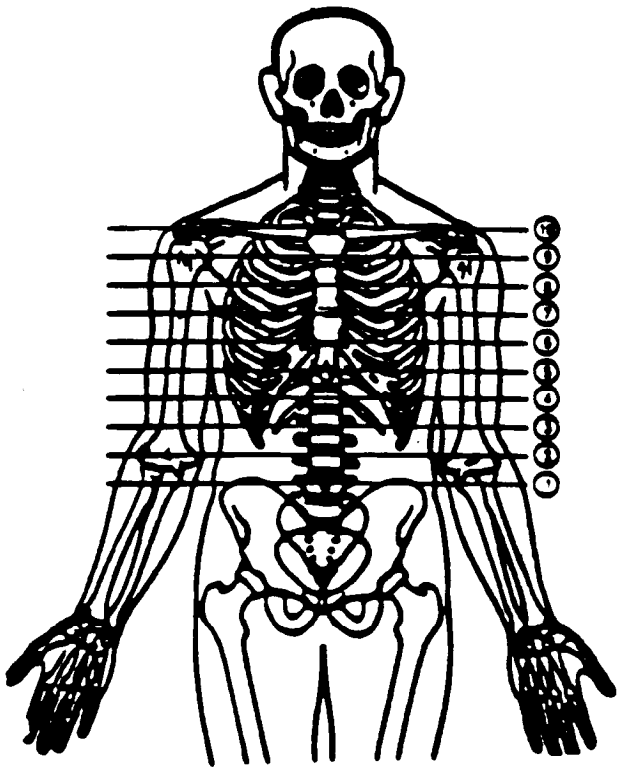

Figure 10. Possible Chest Band's locations on the Human Thorax

An attempt was made to try to map the location of the rib fractures on the Max. Dk vs. S curve in Figure 11. It shows that the rib fractures occurred in region B and C for the top band and only in region B for the bottom band.

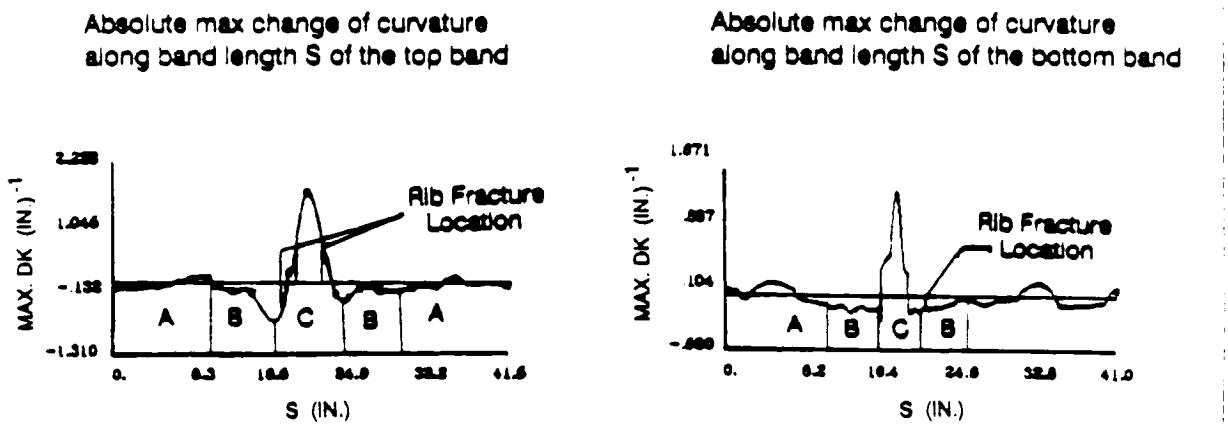

Figure 11. Fracture location mapping on the Absolute change of Curvature from Medical College of Wisconsin Data.

The second test was performed by the University of Heidelberg (HDL). The cadaver was 36 years old. In this particular test only one 16-gauge chest band was used at level 7. The autopsy/ report indicates that there was no rib fractures. The absolute maximum change of curvature along the band length for this test is shown in Figure 12.

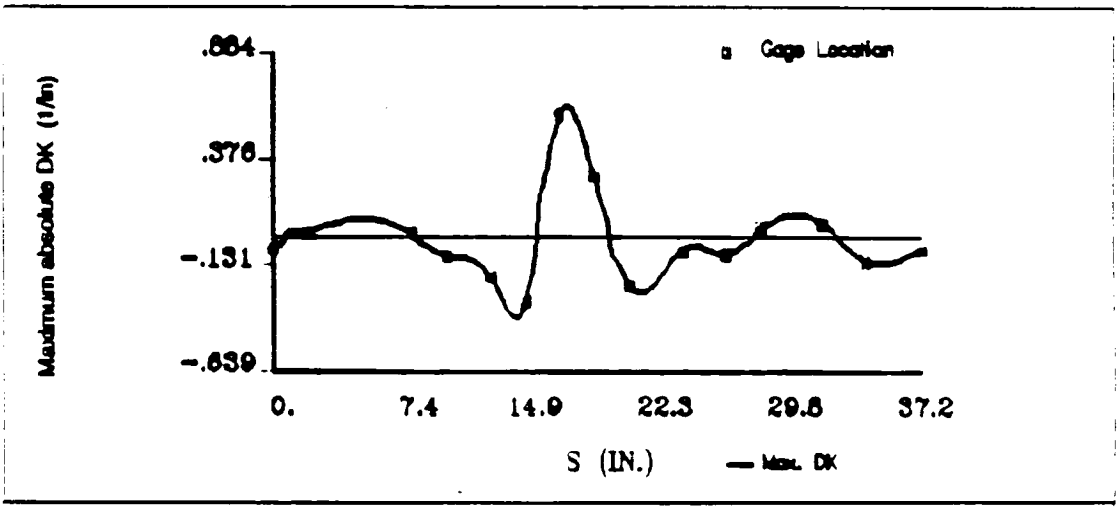

Figure 12. Maximum change of curvature of a No Rib Fracture Case (Heidelberg's Data)

Figure 13 compares the Max. DK vs. S curves of the corresponding top bands from each test. This shows that the magnitude of the max. DK in nearly all regions is much higher in the injury case than the no-injury one.

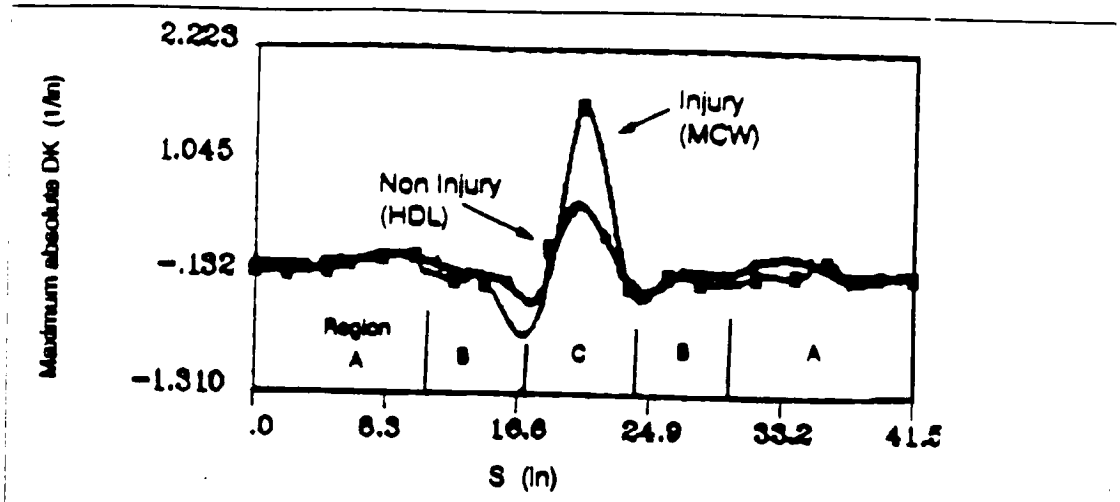

Figure 13. Comparison of maximum absolute change of curvature between injury (Medical College of Wisconsin) and non injury (Heidelberg) cases

Developing a New Thoracic Internal Injury Criterion Using The Chest Band Data

In the past, analytical approaches to develop a thoracic injury criterion have been limited to used of either deformation, as implied in deflection based criteria [4,5,6,7] or the inertial motion of the thorax, as indicated by the acceleration based criterion [3]. With the invention of the chestband by Eppinger [1], an instrument is now available which can accurately measure chest deformation so that it is no longer necessary to rely upon only one chest deflection measurement to characterize the deformation of the thorax. With the advantage of a complete peripheral description of deformation, a new and more complete way of developing an injury criterion can be pursued.

The Stress Analysis Methodology

The injury or failure of structures internal to the thorax experiencing an impact can be attributed to those structure experiencing conditions that exceed their individual critical stress or strain thresholds. Since the actual stresses and strains are a direct result of the deformations and motions that the surface of the thorax undergoes, it appears, at least theoretically, that if one has information about the deformation and motion of the surface of the body, that the internal stresses and strain can be determined and ultimately interpreted to predict the occurrence and extent of internal injuries.

The process proposed to accomplish this is to first create a finite element model of the thorax. Then stimulate this model using the deformations as determined by the

chestband and inertial motions as determined by accelerometry. The output of the model, local stress and strains, are then examined to establish correlation between them and observed injury and non-injury areas.

To establish the feasibility of this concept, a simplified model of the thorax was developed. This model represents the thorax as a one-inch thick viscoelastic material slab whose contours correspond to the actual undeformed thorax of the cadaver specimens as captured by the chestband instrument. The finite element mesh of this simplified chest model is given in Figure 14. It consists of 1805 nodes and 1360 three-dimensional 8-node shell elements. The model's constitutive properties are given in Table 1.

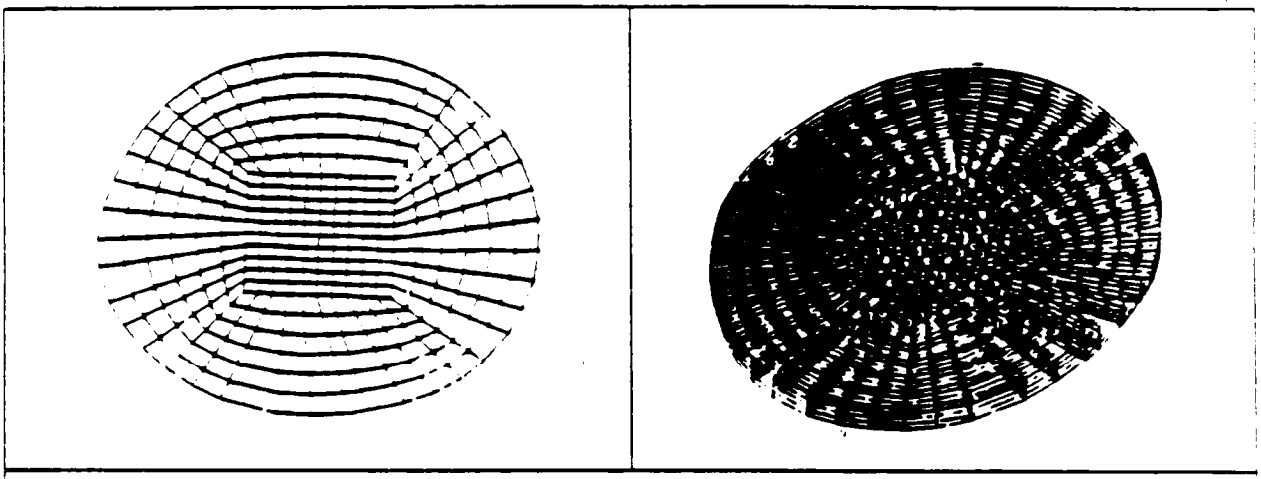

Figure 14. The finite element mesh of a simplified one inch thick viscoelastic chest model

Peripheral deformations and inertial motions as determined from the output of the chestband and accelerometers used in actual tests were processed to be compatible input to the finite element model. The model was then stimulated by these motions and the internal stress contours produced.

Conditions of The Analyticals Simulations

Nodal boundary conditions for the chest model were generated for two reasons. First, to evaluate the feasibility of stimulating a finite element model using experimentally measured boundary deformations and, secondly, to investigate if experimentally measured deformation alone is sufficient to determine internal stresses or must the deformation be accompanied by the total inertial motions the body experiences. To simulate the first condition, the model was driven by the nodal deflection time histories measured experimentally. However, the inertial effects due to body motion are set to be negligible by making the sternum stationary with respect to inertial reference frame of the simulation. The nodal deflection time histories were computed from the times series of deformed contours of the subject thorax captured by the chestband instrument. The continuous nodal deflection time history function was derived by

applying a cubic spline curve fitting technique to the discretized nodal displacement time history developed from the chest band. Because the DYNA3D program accepts only nodal velocity time histories, the nodal deflection time history were converted to velocity time histories by a simple derivative algorithm. Examples of both a nodal displacement and its corresponding velocity time history are shown in figure 15a and 15b.

To simulate the second case where the effect of measured inertial motion of the body is taken into account, the sternal velocity, derived from the experimentally measured sternal acceleration, was added to each previously derived nodal velocity. The total nodal velocity time history at each boundary node then consists of the summation of the nodal velocity from the deformation as computed in the first case plus the velocity derived from the sternum acceleration. An example of some of these nodal velocity time histories is given in Figure 15c.

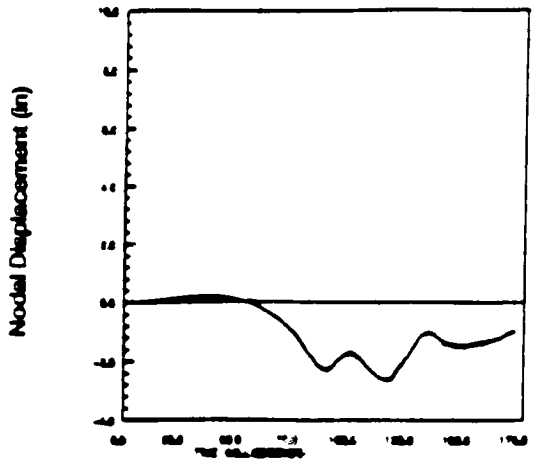

Figure 15a

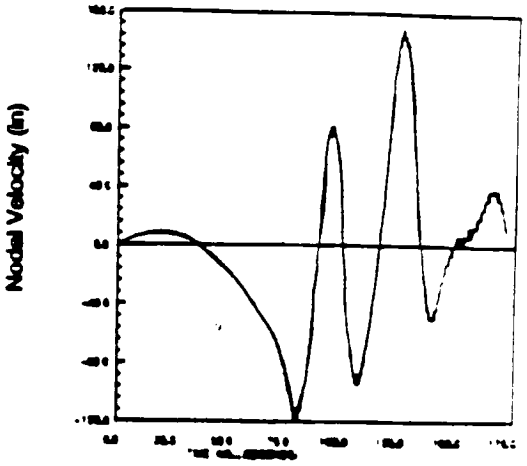

Figure 15b

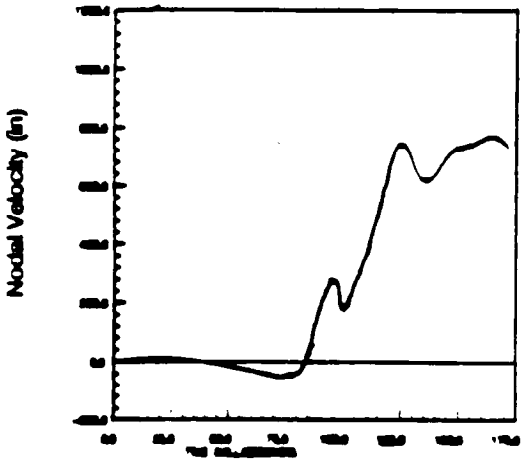

Figure 15c

15a. Nodal dispalcement of a boundary node

15b. Nodal velocity of a boundary node without inertial effect

15c. Nodal velocity of a boundary node with inertial effect

Figure 15. An example of nodal displacement and velocity time history of boundary node derived from chest band data.

As a result of this procedure, the thoracic model experiences exactly the same deformation pattern in both simulations and only the latter simulation experiences the additional of the gross inertial effects. The stress analysis on the two chest band data sets used in section one is carried out both with and without inertial effects.

Results From The Two Simulations:

Relative Displacement and Velocity

Four node locations inside the chest model, two each in the vicinity of the spine and the sternum, are chosen from each simulation (See Figure 16). To analyze the relative displacement and velocity, each of the nodes near the spine is paired with a node near the sternum which is closely aligned in the anterior-posterior direction. The relative displacement and velocity between the two nodes in each pair is then plotted for the time history of the event (See Figures 17 to 20). Each figure shows the result both with and without inertial effects. In both cases, the displacement and velocity are higher when inertial effects are included. (It is also worth noting the difference between the two data sets. The results in the Wisconsin (injury) data show much larger differences than in the Heidelberg(non-injury) data.)

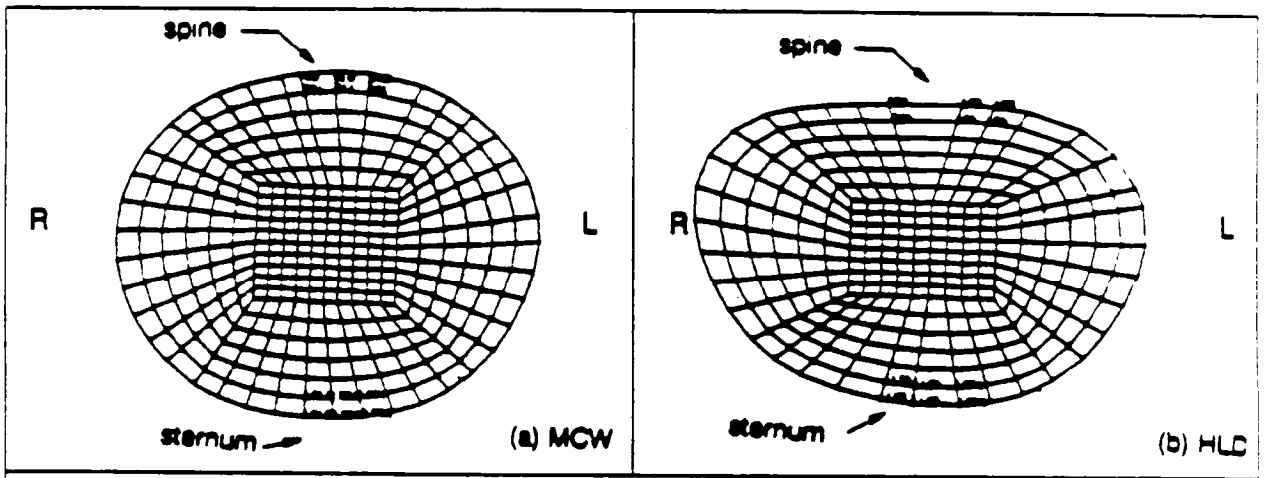

Figure 16. Peripheral nodes around the spine and the sternum. MCW = Medical College of Wisconsin HDL = Heidelberg

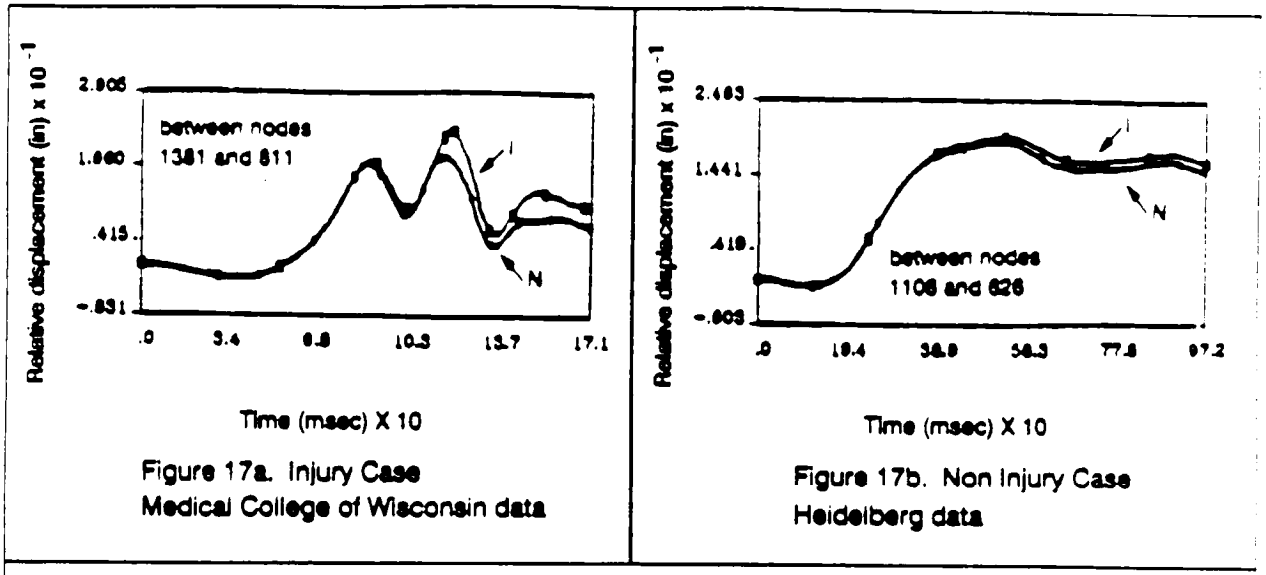

Figure 17a. Injury Case
Medical College of Wisconsin data

Figure 17b. Non Injury Case
Heidelberg data

Figure 17. Relative displacement time history in anterior-posterior direction

I = with inertial effect
N = without inertial effect

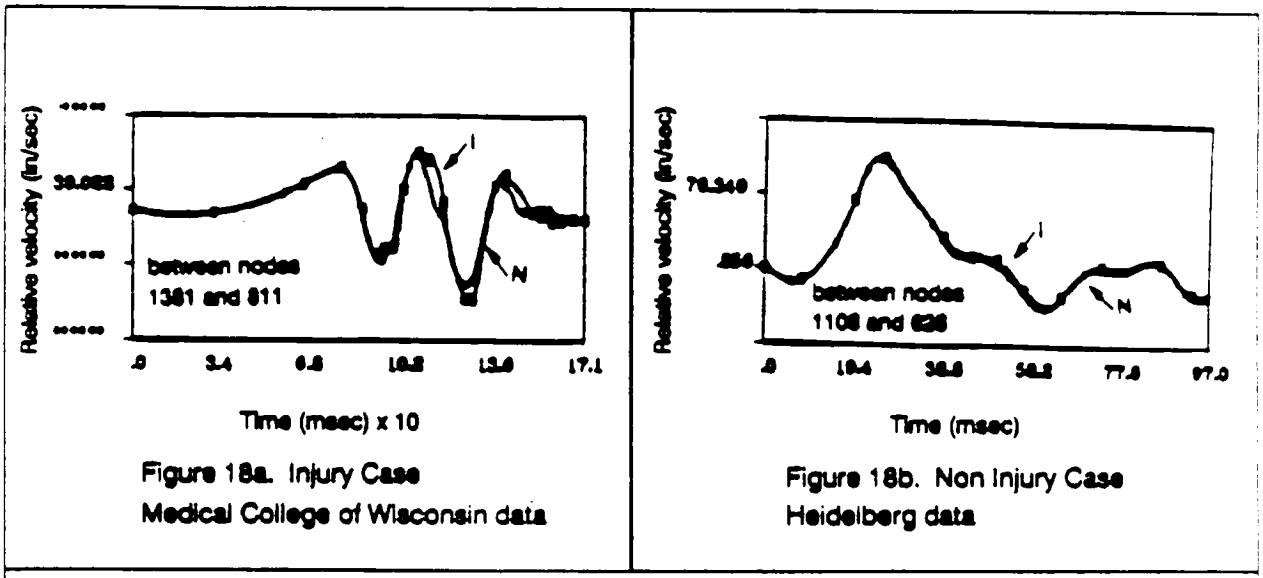

Figure 18a. Injury Case
Medical College of Wisconsin data

Figure 18b. Non Injury Case
Heidelberg data

Figure 18. Relative velocity time history in anterior-posterior direction

I = with inertial effect
N = without inertial effect

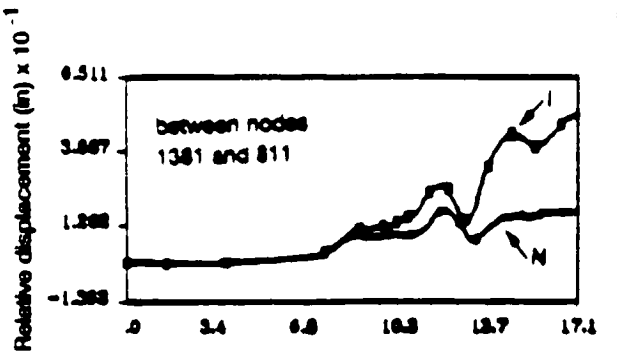

Figure 19a. Injury Case
Medical College of Wisconsin data

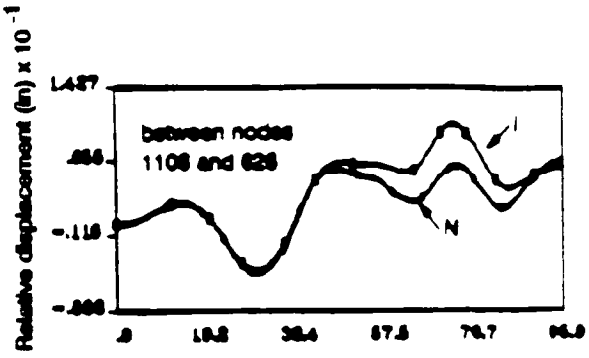

Figure 19b. Non Injury Case
Heidelberg data

Figure 19. Relative displacement time history in left-right direction

I = with inertial effect
N = without inertial effect

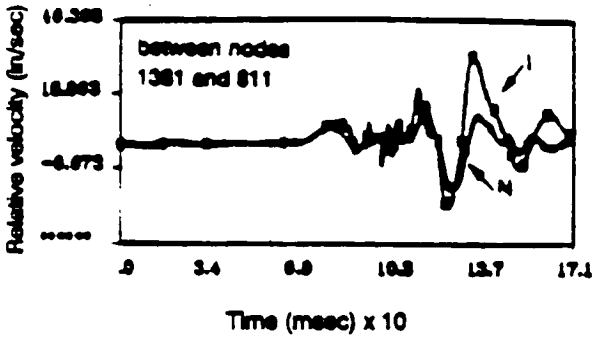

Figure 20a. Injury Case
Medical College of Wisconsin data

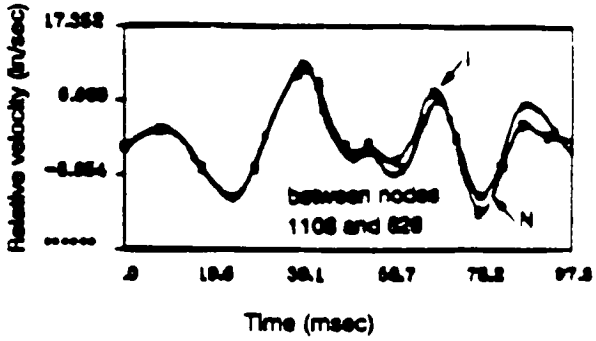

Figure 20b. Non Injury Case
Heidelberg data

Figure 20. Relative velocity time history in left-right direction

I = with inertial effect
N = without inertial effect

Maximum and Minimum Pressure

Figures 21a,b and 22a,b show the maximum and minimum pressure respectively. Each curve represents the maximum or minimum pressure at each time step irrespective of its location within the chest model. For each time step the location of the maximum/or minimum pressure between the two cases, namely with and without inertial effect, always occur at the same point inside the chest model. Once again the addition of the inertial effects results in higher maximum and minimum values.

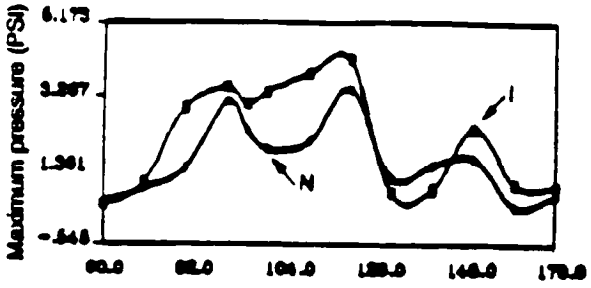

Figure 21a. Injury Case
Medical College of Wisconsin data

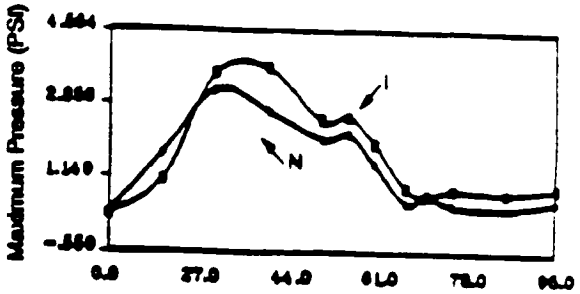

Figure 21b. Non Injury Case
Heidelberg data

Figure 21. Maximum pressure inside the chest models

I = with inertial effect
N = without inertial effect

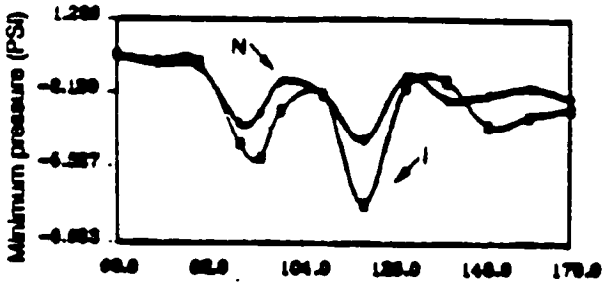

Figure 22a. Injury Case
Medical College of Wisconsin data

Figure 22b. Non Injury Case
Heidelberg data

Figure 22. Minimum pressure inside the chest models

I = with inertial effect
N = without inertial effect

Maximum Von Mises Effective Stress and Strain

Figures 23a,b and 24a,b show the maximum Von Mises [9] effective stress and strain respectively. As in the the pressure plots each curve represents the maximum stress or strain at each time step irrespective of its location. But at each time step the location of its occurrence inside the chest model from both cases is always the same. Here also, the result of adding inertial effects is higher stress or strain values.

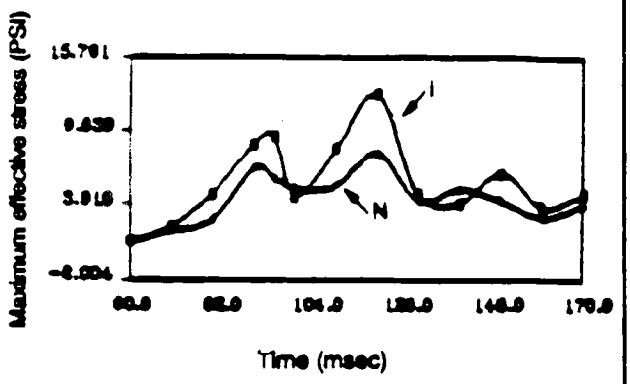

Figure 23a. Injury Case
Medical College of Wisconsin data

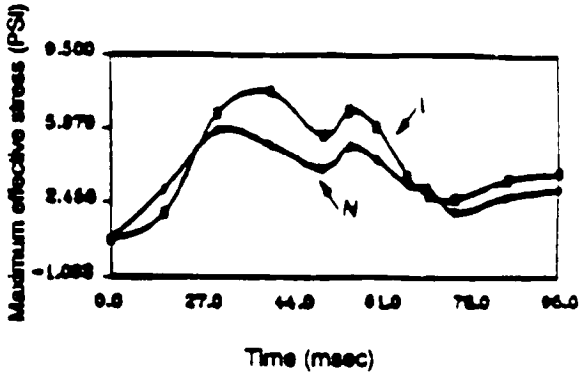

Figure 23b. Non Injury Case
Heidelberg data

Figure 23. Maximum Von Mises effective stress time history inside the chest model

I = with inertial effect
N = without inertial effect

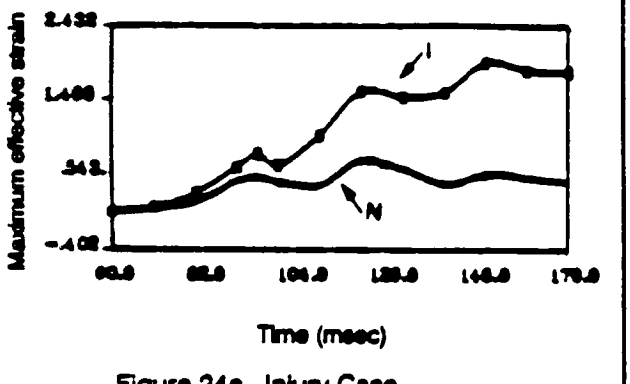

Figure 24a. Injury Case
Medical College of Wisconsin data

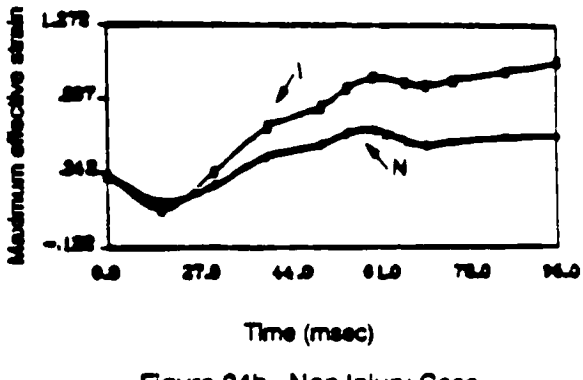

Figure 24b. Non Injury Case
Heidelberg data

Figure 24. Maximum Von Mises effective strain time history inside the chest model

I = with inertial effect
N = without inertial effect

Conclusions

With the advent of the EPIDM chest band, a much more complete description of the mechanical effects of crash forces on the human thorax can be obtained. This more complete description has the potential of effecting development of more accurate injury predictive methodologies which utilize this information. It appears that the prediction of thoracic rib failure is the most straight forward to accomplish because parameters, local curvature, which are a direct output of the EPIDM process can be theoretically and experimentally linked to failure. Examples of how this would be accomplished have been presented and it now remains to acquire sufficient experimental data in order to establish the critical threshold values for the various areas of the chest.

The EPIDM process also appears to allow the development of a procedure which has the capabilities of predicting internal thoracic injuries. The process of analytically analyzing the effects of experimentally obtained deformational and inertial motions on a model of a thorax has been shown to be feasible and practicable. Initial investigations have strongly suggested that when additional experimental efforts are undertaken to establish the data base from which any criteria is to be developed, that both the deformation and inertial data are necessary to accurately predict the true stresses and strains, and therefore the injuries that are occurring within the thorax.

Table 1
Material Properties for Simplified One-Inch Thick Viscoelastic Thorax Model.

The Viscoelastic model used in DYNA3D is represented by the following relaxation function:

$$G(t) = Gl + (Gs - Gl)e^{-(BETA)t}$$

where:

Gs = Short term shear modulus.
Gl = Long term shear modulus.
BETA = Decay constant.
t = Time

Material Properties Used in the Stress Analysis

Gs = 10.4 psi
Gl = 0.3425 psi
Beta = 100
Density = 0.75 x10.0e-4 Lb Mass / (in)**3
Bulk Modulus = 100.0 psi

Disclaimer

The views presented are those of the authors and are not necessarily those of the National Highway Traffic Safety Administration, U. S. Department of Transportation.

References

1. Eppinger R.H.: On the Development of a Deformation Measurement System and Its Application Toward Developing Mechanically Based Injury Indices. Proceedings of the 33th STAPP Car Crash Conference. pp 21-28,1989. Washington ,DC.

2. Yamada, H.: Strength of Biological Materials. Edited by F. G. Evans. The Williams & Wilkins Company, Baltimore 1970.

3. Eppinger R.H.,Marcus J.H.,Morgan R.M.: Development of Dummy and Injury Index for NHTSA's Thoracic Side Impact Protection Research Program. SAE Technical Paper Series # 840885.

4. Stapp J.P.: Voluntary Human Tolerance Levels. In Impact Injury and Crash Protection. Gurdjian E.S, Lange W.A., Patrick L.M., Thomas L.M. (Editors), Charles C. Thomas, Springfield,Illinois.

5. Kroell C.K., Schneider D.C, Nahum A.M.: Impact Tolerance and Response of the Human Thorax II. 18th STAPP Car Crash Conference SAE, Warrendale, PA 1981.

6. Neathery R.F.: An Analysis of Chest Impact Response Data and Scaled Performance Recommendations. Proceedings of the 18th STAPP Car Crash Conference.

7. Lau I.V, Viano D.C.: The Viscous Criterion- Base and Applications of an Injury Severity Index for Soft Tissues. Proceedings of the 30th STAPP Car Crash Conference.

8. Hagedorn A.V., Eppenger R.H., Morgan R.M., Pritz H.B., Khaewpong N.: Application of a Deformation Measurement System to Biomechanical Systems. Proceedings of the 1991 International IRCOBI Conference, Berlin (Germany).

9. Fung Y.C.: Foundation of Solid Mechanics. Prentice-Hall International Series in Dynamics.